

Weak itinerant-electron ferromagnetism in Ni-rich Ni-Fe-Cr and Ni-Fe-V alloys

A. K. Gangopadhyay, R. K. Ray, and A. K. Majumdar

Department of Physics, Indian Institute of Technology, Kanpur 208016, Uttar Pradesh, India

(Received 14 March 1984)

Detailed magnetization measurements have been carried out for a number of alloys in both the ternary series Ni-Fe-Cr and Ni-Fe-V in the Ni-rich region, mainly to study the effect of the addition of Cr or V. The following points emerge from the measurements in the ferromagnetic as well as paramagnetic range of temperatures: (i) The low-temperature magnetization data reveal that in Ni-Fe-Cr alloys, along with the spin waves, Stoner single-particle excitation corresponding to weak itinerant-electron ferromagnets (following a T^2 law) is present. The Stoner term gains prominence with increasing Cr concentration. In Ni-Fe-V alloys there is also some indication of the existence of other than spin-wave excitations. (ii) The variation of $\bar{\mu}$ (average number of Bohr magnetons per atom) with concentration shows the same type of nonlinearity in both systems, in agreement with the earlier data of Men'shikov *et al.* on Ni-Fe-Cr alloys. (iii) Magnetization falls much faster with temperature than in conventional ferromagnets (e.g., Ni,Fe) over the entire ferromagnetic region. (iv) The Rhodes-Wohlfarth ratio (q_c/q_s) shows a rapid increase with increasing concentration of Cr or V (i.e., with decreasing T_c) and Arrott plots of the Cr- or V-rich alloys are linear over a large temperature range. From the above observations we conclude that the addition of Cr or V in Ni-Fe alloys moves them towards weak itinerant-electron ferromagnetism.

I. INTRODUCTION

Recently, much interest has been attracted by a number of alloy systems where some of the exchange interactions are ferromagnetic and some antiferromagnetic in nature. A host of interesting magnetic phases has been observed in these systems, viz., the spin-glass phase, the mixed magnetic phase (where the high-temperature phase is ferromagnetic and the low-temperature phase is a mixture of ferromagnetic and spin-glass phases), etc. The ternary Ni-Fe-Cr system is one of this type, and has recently been studied by Men'shikov and Teplykh,¹ and also by Majumdar and Blanckenhagen.² However, their studies were limited mainly to the Fe-rich region. In the Ni-rich region, except for the measurements of spin-wave-stiffness constant by neutron scattering³ and variation of average number of Bohr magnetons per atom with composition,^{1,3} not much work has been done so far. Therefore we thought it would be interesting to study this region, especially to see the influence of Cr on the magnetization behavior as a function of temperature. As a parallel system, we also selected Ni-Fe-V alloys to make a comparative study of the influence of Cr or V in Ni-Fe alloys.

With the above ideas in mind, we have made detailed magnetization measurements from 77 K to room temperature, and for a few alloys, even up to T_c and above. The low-temperature data could be explained in terms of the conventional spin-wave theory only when a higher-order term (which, in our case, is $T^{7/2}$ or T^4) is included. However, even then the spin-wave-stiffness constant values for all the alloys (Ni-Fe-Cr) studied have been found to be less than the corresponding neutron-scattering values. This difference could be explained as being due to the existence of single-particle excitations, following a T^2 law, but the contribution of this Stoner term is enhanced as the Cr

concentration is increased. In the case of the V series, the presence of such a term could not be established because of the absence of any such neutron-scattering data. The average number of Bohr magnetons per atom ($\bar{\mu}$) found from the extrapolation of the low-temperature data to 0 K showed a similar type of nonlinear composition dependence in the two systems, and essentially followed the earlier results of Men'shikov *et al.*³ on Ni-Fe-Cr system. The nonlinearity, however, could not be explained in terms of conventional theories. Furthermore, saturation magnetization for alloys in both series have been found to decrease faster with temperature than those in conventional Heisenberg ferromagnets.

The above results prompted us to study the paramagnetic region for some of the Cr- or V-rich alloys. It was observed that the Curie-Weiss law is obeyed, but at temperatures much higher than T_c , and the effective Bohr magnetons per atom found from the Curie constant are always larger than those obtained from the low-temperature magnetization data. Inspired by this, we have tried to explain our data in terms of itinerant-electron models and have found that the Cr- or V-rich ternary alloys in both series fit better into the itinerant-electron model than the localized ones.

II. EXPERIMENTAL PROCEDURE

A number of alloys in both ternary series (Cr and V) were prepared by induction melting of the required amount of constituents of Johnson-Mathey, Inc. Spec-pure-grade materials. The ingots were homogenized at 1100°C for 48 h in an argon atmosphere, and after obtaining samples of the required shape (cylindrical) and size, they were finally annealed at 900°C for 24 h, and water-

quenched. The actual composition of the samples was checked by spectroscopic methods, and in a few cases also by chemical analysis.

All magnetic measurements were carried out by a Princeton Applied Research model 155 vibrating-sample magnetometer (VSM). A model 153 variable-temperature cryostat, or a model 151 high-temperature oven assembly, in conjunction with the VSM, enabled us to extend our measurements, respectively, in the low- (from 77 to 300 K) or high- (above 300 K) temperature regions. The sample temperature was read by using a Chromel-Alumel thermocouple in the high-temperature region, and by using a gallium-arsenide diode as well as a copper-Constantan thermocouple at low temperatures. Calibration of the VSM was always done with respect to a standard Ni sample, and magnetic fields (up to 18 kOe) were provided by a 15-in. Varian Associates electromagnet. By suitable choice of the samples' mass, a change in magnetic moment could be detected up to 2 parts in 10^4 .

Curie temperatures were determined from the rate of fall of magnetization as a function of temperature in the residual field (~ 30 Oe) of the electromagnet. The values of T_c and other parameters presented here are the averages over several measurements of the same piece, and wherever necessary, on different pieces of the same sample. The details of measurements of other quantities will be discussed along with the presentation of the data in Sec. III.

III. RESULTS AND DISCUSSION

A. Low-temperature magnetization data for Ni-Fe-Cr alloys

1. Spin-wave analysis

It is well known that, in ferromagnets, in the long-wavelength limit, the spin-wave energy (ϵ) is related to the wave vector (q) by

$$\epsilon(q) = g\mu_B H_{\text{int}} + Dq^2 + Eq^4 + \dots, \quad (1)$$

where the first term manifests itself as an energy gap in the presence of an effective internal field H_{int} , arising from the applied field, the anisotropy field, and the Lorentzian or the spin-wave demagnetizing field. D is the usual spin-wave-stiffness constant and E is the constant of proportionality for the q^4 term.

At low temperatures, due to the spin-wave excitations, the specific magnetization σ (in units of emu/g), in the presence of an external magnetic field H , decreases by⁴

$$\begin{aligned} \frac{\Delta\sigma(H, T)}{\sigma(0, 0)} &= \frac{\sigma(H, T) - \sigma(0, 0)}{\sigma(0, 0)} \\ &= \alpha' z \left[\frac{3}{2}, \frac{T_g}{T} \right] T^{3/2} + \beta z \left[\frac{5}{2}, \frac{T_g}{T} \right] T^{5/2} + \dots, \end{aligned} \quad (2)$$

where $T_g (= g\mu_B H_{\text{int}}/k_B)$ is the gap temperature, giving rise to the two correction terms

$$z \left[\frac{3}{2}, \frac{T_g}{T} \right] \quad \text{and} \quad z \left[\frac{5}{2}, \frac{T_g}{T} \right]^5,$$

and α', β are two constants involving D , etc. Basically, the $T^{3/2}$ term in Eq. (2) originates from the harmonic (q^2) term in the spin-wave dispersion relationship, and the $T^{5/2}$ term has its origin in the anharmonic (q^4) term. Because of the temperature dependence of D , some additional higher-order terms may also enter, depending on the relationship between D and the temperature T . According to the localized models of Dyson⁶ and others,⁷ at low temperatures magnon-magnon interactions can give rise to a leading $T^{5/2}$ term in D in the long-wavelength limit. On the other hand, itinerant models of Izuyama and Kubo⁸ and others⁹ predict a $T^{5/2}$ term due to magnon-magnon interaction and a T^2 term due to the interaction between spin waves and thermally excited itinerant electrons. Thus, in the low-temperature limit,

$$D = D_0(1 - D_1 T^2 - D_2 T^{5/2}). \quad (3)$$

Inelastic long-wavelength neutron-scattering experiments on Fe (Ref. 10) have shown the presence of both terms, but with D_2 negative, whereas experiments on Ni (Refs. 11–13) indicate the presence of a single term, namely T^2 . Substitution of Eq. (3) in (2) gives

$$\begin{aligned} \frac{\Delta\sigma(H, T)}{\sigma(0, 0)} &= \alpha T^{3/2} (1 - D_1 T^2 - D_2 T^{5/2})^{-3/2} z \left[\frac{3}{2}, \frac{T_g}{T} \right] \\ &\quad + \beta z \left[\frac{5}{2}, \frac{T_g}{T} \right] T^{5/2}, \end{aligned} \quad (4)$$

where

$$\alpha = \alpha'(D = D_0) = \left[\frac{k_B}{4\pi D_0} \right]^{3/2} \frac{2.612g\mu_B}{\sigma(0, 0)\rho}, \quad (5)$$

and

$$\beta = \frac{3k_B}{16} \langle r^2 \rangle \frac{\alpha}{1.948D_0}, \quad (6)$$

with ρ as the density and $\langle r^2 \rangle$ the mean-square range of the exchange interaction. The other symbols carry their usual meanings. A binomial expansion of the first term, in small parentheses, of Eq. (4) generates a $T^{7/2}$ term and/or a T^4 term. To summarize, in addition to the $T^{3/2}$ term, one can have (i) a $T^{5/2}$ term in the presence of an anharmonic term (q^4) in the spin-wave dispersion relationship, and (ii) a $T^{7/2}$ term and/or a T^4 term, depending on the temperature dependence of D .

The low-temperature magnetization data, measured at 5 K intervals from 77 K upwards in a constant magnetic field of 8 kOe for a number of Ni-Fe-Cr alloys, were analyzed in terms of the above theory. Measurements below 77 K could not be extended because of the lack of such a facility at the present. Thus, only alloys having sufficiently high T_c (~ 500 K and above) were chosen and our analysis was confined to data below $0.5T_c$ in order to render the spin-wave analysis meaningful. Least-squares fits to Eq. (4) were tried using various unknown parameters, taking three at a time, viz., $\sigma(0, 0)$, α , and one of the higher-order terms. Inclusion of more than three parameters was not possible as it often led to an unphysical situation where the coefficients of some of the higher-order

terms turned out to be positive. We believe that this is because the inclusion of so many parameters demanded more from our experimental data than what their limited accuracy could permit.

The correction factors due to the finite applied field, viz.,

$$Z \left[\frac{3}{2}, \frac{T_g}{T} \right] \text{ and } Z \left[\frac{5}{2}, \frac{T_g}{T} \right],$$

were calculated at each temperature using a series expansion in powers of T_g/T as given by Argyle *et al.*⁵ However, since the magnetocrystalline anisotropy is not known for these alloys, and there is some uncertainty in calculating the demagnetizing field, the exact value of T_g could not be calculated. To circumvent this difficulty, T_g was itself taken as a parameter, and the T_g value that gave the best fit was taken. In Table I we give the results of such an analysis for one of our samples. The standard deviations (SD) of the least-squares fits are also included and the values of the various parameters are given along with their statistical uncertainties. It is amply clear from Table I that inclusion of higher-order terms other than $T^{3/2}$ is essential. The minimum SD could be achieved when a $T^{7/2}$ (or T^4) term is included along with the $T^{3/2}$ term. A better fit with a $T^{7/2}$ (or T^4) term rather than a $T^{5/2}$ term clearly indicates that the deviation from the $T^{3/2}$ law comes mainly from the temperature dependence of the spin-wave-stiffness constant rather than the anharmonicity term in the spin-wave dispersion relation. An attempt to include both the $T^{7/2}$ (or T^4) term and a possible $T^{5/2}$ term along with the usual coefficients $\sigma(0,0)$ and α proved to be futile for reasons discussed earlier. It seems that even if it exists, the $T^{5/2}$ term plays only a minor role compared to the $T^{7/2}$ (or T^4) term. This is consistent with the inelastic-neutron-scattering studies in Ni-Fe-Cr alloys by Men'shikov *et al.*,³ in which they have not reported the presence of any term higher than quadratic in the spin-wave dispersion relation. However, the presence of such a term in binary Ni-Fe alloys detected from magnetization^{14,15} as well as from neutron-scattering measurements¹⁶ suggests that the addition of Cr in Ni-Fe alloys probably suppresses the anharmonic term.

A similar analysis was carried out for all the alloys studied, and it was found that a $T^{3/2}$ term along with a $T^{7/2}$ (or T^4) term gave the best fit to our experimental data. A distinction between a $T^{7/2}$ and a T^4 term could not be made since both of them gave an almost equally good fit. However, recent magnetization studies,¹⁴ as well as neutron-scattering measurements,^{17,18} reveal that $D \propto T^{5/2}$ in the Ni-rich region of binary Ni-Fe alloys. Guided by these data it seemed logical to accept the T^4 term as the next-higher-order term instead of a $T^{7/2}$ term in these Ni-rich ternary alloys.

In Fig. 1 we show the changes in the reduced magnetization as a function of reduced temperature (T/T_c). The solid curves are the best fits with $\sigma(0,0)$, α , and γ (coefficient of the T^4 term) as the adjustable parameters, and we present the corresponding parameter values in Table II. The spin-wave-stiffness constants D_0 and D_2 , derived from the coefficients α and γ , are also presented in the

TABLE I. Results of various least-squares fits of magnetization vs temperature data, taken at a fixed field of 8 kOe for sample no. 26.

Sample composition (at. %)	Temperature range in which data have been analyzed	$\sigma(0,0)$ (emu/g)	α ($10^{-5} \text{ K}^{-3/2}$)	β ($10^{-8} \text{ K}^{-5/2}$)	Coefficient of $T^{7/2}$ term ($10^{-10} \text{ K}^{-7/2}$)	Coefficient (γ) of T^4 term (10^{-12} K^{-4})	Standard deviation of least-squares fits of $\Delta\sigma/\sigma$ (10^{-4})
Ni ₈₀ Fe ₁₆ Cr ₄	0.12 T_c	79.03 ± 0.04	-(1.63 ± 0.03)				10.9
	78.40 ± 0.02	-(0.33 ± 0.04)	-(4.60 ± 0.14)				1.7
	to						
	0.33 T_c	78.57 ± 0.01	-(0.97 ± 0.014)		-(1.08 ± 0.02)		1.2
	78.62 ± 0.01	-(1.09 ± 0.01)				-(5.92 ± 0.12)	1.15

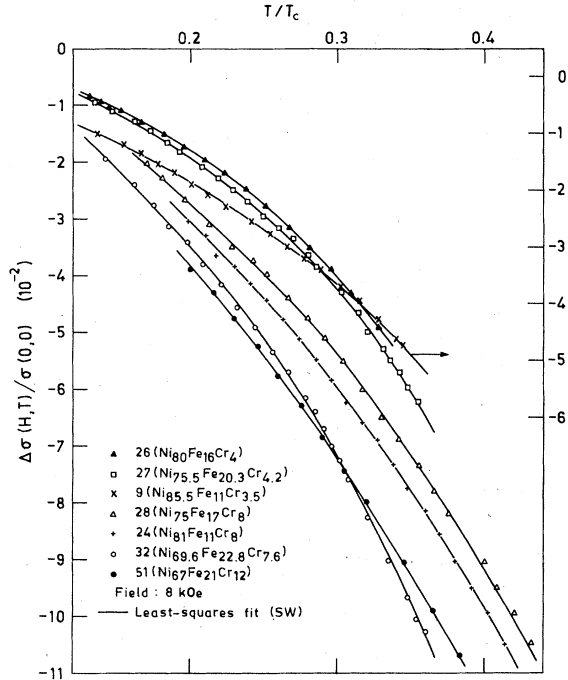


FIG. 1. Change of reduced magnetization ($\Delta\sigma/\sigma$) as a function of reduced temperature (T/T_c) for various Ni-Fe-Cr alloys. The solid lines are the least-squares fits of the experimental data according to spin-wave theory.

table, along with the estimated values of D_0 obtained from the neutron-scattering data of Men'shikov *et al.*³ In the calculations for our D_0 , the g values were taken to be 2 and the densities ρ were calculated using the lattice-parameter data of Men'shikov *et al.*³ Actual measurements of density for a few alloys have shown that the calculated values of ρ are within 1% of the measured ones. The following points emerge from the results shown in Table II:

(i) Although spin-wave theory can account for the change in magnetization with temperature over a fairly wide range of temperature very well (see Fig. 1), the D_0 values determined from magnetization measurements are always less than the corresponding neutron-scattering values—at least for the alloys studied.

(ii) Although they are in disagreement with neutron-scattering results, our magnetic-measurement-based values for D_0 essentially show the same kind of compositional dependence. For the alloys with fixed Cr concentration, after showing an initial increase, D_0 falls off with increasing Fe concentration. However, with the addition of Cr, D_0 continuously falls off at a much faster rate. This finds a qualitative explanation in the observation of Men'shikov *et al.*³ that the Cr-Cr interaction is antiferromagnetic and strongest (~ 227 meV) among all of the pair interactions in Ni-Fe-Cr alloys. The Fe-Fe interaction is also antiferromagnetic, but much weaker (~ 7 meV) in strength, so that its effect can play a major role only when the Fe concentration is relatively high. Thus, addition of even a few atomic percent of Cr could reduce the effective exchange interaction by a considerable

TABLE II. Results of the least-squares fit for the temperature dependence of magnetization for some Ni-Fe-Cr alloys. The statistical uncertainty in the various parameters is also included.

Sample no.	Composition of Ni-Fe-Cr alloys (at. %)	Density ρ^a (g/cm ³)	$\sigma(0,0)$ (emu/g)	$-\alpha$ (10^{-5} K ^{-3/2})	$-\gamma$ (10^{-12} K ⁻⁴)	D_0 (meV Å ²)	D_2 (10^{-7} K ^{-5/2})	D_0 from neutron scattering (meV Å ²)	Standard deviation of least-squares fit of $\Delta\sigma/\tau$ (10^{-4})
9	85.5-11-3.5	8.69	65.38±0.02	1.46±0.03	2.6±0.3	222±12	2.7±0.4	310 ^b	3.0
24	81-11-8	8.65	52.95±0.03	3.99±0.05	7.2±0.5	131±8	1.2±0.1	180 ^c	4.9
26	80-16-4	8.63	78.62±0.01	1.09±0.01	5.9±0.1	239±14	3.6±0.1	315 ^b	1.1
28	75-17-8	8.56	66.46±0.08	2.64±0.1	7.0±0.7	150±10	1.8±0.3	200 ^c	10
27	75.5-20.3-4.2	8.61	86.54±0.03	1.11±0.02	5.3±0.2	223±15	3.2±0.2	320 ^b	3.2
32	69.6-22.8-7.6	8.50	80.21±0.05	2.58±0.06	8.9±0.6	135±10	2.3±0.2	210 ^c	5.9
51	67-21-12	8.42	61.76±0.02	4.77±0.03	2.8±0.3	107±7	0.4±0.05		3.8

^a ρ values were calculated.

^bValues estimated from Fig. 3 of Ref. 3.

^cValues directly from Fig. 3 of Ref. 3.

amount and thereby reduce D_0 .

(iii) As Cr is added, α increases much faster than γ . This implies that the $T^{3/2}$ law should hold over a larger range of temperature (in the scale of T/T_c) for the Cr-rich alloys. This is exactly what was observed when $\Delta\sigma/\sigma$ was plotted against $T^{3/2}$ (not shown). Actually, this is one of the reasons why spin-wave analysis is meaningful even with the data above 77 K for this alloy system. It is also important to mention that this kind of behavior has been observed in a large number of amorphous ferromagnets.¹⁹

(iv) Although the absolute values of D_2 are slightly uncertain, they show a systematic trend of falling with increasing Cr concentration. This is similar to the behavior found in Ni-Fe alloys, where D_2 decreases with increasing Fe concentration.^{14,17,18} The rate of decrease with the addition of Cr, however, is much faster than those found due to the addition of Fe in binary Ni-Fe alloys.

One might wonder whether the discrepancy in the D_0 values obtained from the magnetization and neutron-scattering experiments is a result of only using data above 77 K (which is more than $0.1T_c$ for all the alloys studied) for our analysis. To check this point we reanalyzed some of the raw magnetization data of Majumdar *et al.*²⁰ on metallic glasses (Fe-B-C). The reasons behind choosing their data were twofold: (a) α and T_c for some of their alloys were of nearly the same magnitude as those for our alloys, and (b) the data were readily available. Basically what was done was the following. α was calculated using data, from (i) 10 to 180 K ($\sim 0.3T_c$), and (ii) 80 to 180 K. It was found that the values of α in the two cases differed by not more than 4%, and hence the values of D_0 thus calculated could only differ by about 2.5% (since $D_0 \propto \alpha^{-2/3}$). Thus we estimate that the effect of excluding data below 77 K on D_0 could not be more than 3%, and perhaps even less for the alloys with higher T_c . In fact, our error bars given for D_0 in Table II include this factor along with the contribution from other sources. It is clear in the light of the above discussions that the observed discrepancy between the two values of D_0 is a real one rather than just an artifact of the experiments.

Such a difference among magnetization,¹³ NMR,²¹ and neutron-scattering-based^{12,17} values for D_0 has also been observed in pure Ni. In the case of Fe, however, D_0 values determined from various types of experiments seem to be in complete agreement.²² Among the crystalline alloys, Fe-Cr (Ref. 23) shows such an anomaly, whereas in amorphous ferromagnets¹⁹ it seems to be a rule rather than an exception. Since neutron-scattering measurements provide a direct method of measuring D , one should accept these values as the real ones rather than those obtained from bulk magnetization measurements. Thus in our case magnetization measurements show that the low-temperature magnetization decreases faster than what one should expect from spin-wave excitations only. This probably indicates to the existence of other excitations. Aldred,¹³ in connection with Ni, has shown that Stoner's single-particle excitations could account for this additional term. Following the same methodology, we have tried to explain the above discrepancy in our case, as will be shown in the following subsection.

2. Stoner excitation

After the classic paper by Stoner²⁴ on itinerant-electron ferromagnetism, numerous workers^{25,26} have enriched and developed this new approach of band or itinerant-electron ferromagnetism. The basic idea behind this model is that the magnetic electrons, which are itinerant in character, are split into spin-up and spin-down bands, separated by the exchange interaction energy. This splitting is assumed to be proportional to the spontaneous magnetization, and, in the low-temperature range, the decrease in magnetization with temperature is a result of the excitation of electrons from this spin-up to spin-down states. Thompson *et al.*²⁷ have shown that depending on whether the magnetization is due to the electrons (holes) from a single spin band or from both, the temperature dependence of magnetization will be different. For strong (i.e., when one subband is completely full) itinerant-electron ferromagnets, the change in reduced magnetization due to single-particle (SP) or Stoner excitations only is given by

$$\left. \frac{\Delta\sigma(T)}{\sigma(0)} \right|_{\text{SP}} = AT^{3/2} e^{-E/k_B T}, \quad (7)$$

under the assumption of a parabolic band. Here, E is the energy gap between the top of the full subband and the Fermi level E_F ($E/k_B T \gg 1$), and the constant A is related to the band parameters of the material. The exponential decrease of σ can be visualized as a result of the existence of the gap E , which necessitates an activation energy to lift the electrons from the filled spin-up states to the empty spin-down states.

On the other hand, for a weak (i.e., when both subbands are only partially full) itinerant-electron ferromagnet, the change in reduced magnetization is given by

$$\left. \frac{\Delta\sigma(T)}{\sigma(0)} \right|_{\text{SP}} = BT^2, \quad (8)$$

where B is related to various band parameters, such as the density of states at the Fermi level, their derivatives, band splitting, relative magnetization $\xi_0 [(n_\downarrow - n_\uparrow)/n_\downarrow]$, etc. The T^2 dependence is simply a manifestation of fermion excitations due to thermal energy. An additional $T^{3/2}$ term may also arise because of the assumption that the molecular field, which splits the spin-up and spin-down bands, is proportional to the total magnetization, which, in turn, decreases as $T^{3/2}$ due to spin-wave excitation.

To search for the existence of any such (Stoner) term, it appeared impractical to add Eq. (7) or (8) to Eq. (4) and then try for a least-squares fit for the reasons discussed in Sec. III A 1. It appeared more logical to follow the procedure of Aldred¹³ of first calculating the expected change in magnetization due to spin-wave excitation only (SW only), using the neutron-scattering D values and subtracting these from the experimental values, at each temperature. The difference then will simply give the change in magnetization due to single-particle excitations only. In such an analysis, the assumption that the two modes of excitation are independent of each other is implicit, which is justified, at least in the low-temperature region. Thus, as a first step (α)_{SW only} was calculated using the data of

Men'shikov *et al.*³ for D_0 . Unfortunately, due to the absence of any such data for D_2 , some approximations had to be made to calculate $(\gamma)_{\text{SW only}}$. Assuming that D_2 (magnetization) is scaled down in the same manner as D_0 due to the presence of the additional (other than spin-wave) excitation, and recalling that $\gamma/\alpha = \frac{3}{2}D_2$, one can write $(\gamma/\alpha)_{\text{expt}} = (\gamma/\alpha)_{\text{SW only}}$. Since experimental values of α and γ are known, using the above relationship one can calculate $(\gamma)_{\text{SW only}}$ by using the calculated value of $(\alpha)_{\text{SW only}}$. Using these $(\alpha)_{\text{SW only}}$ and $(\gamma)_{\text{SW only}}$ values the decrease in magnetization at each temperature was calculated, and then deducting it from the experimental values, the decrease in σ due to the additional excitation $[\Delta\sigma(T)/\sigma(0)]_{\text{SP}}$, was obtained. The above quantity can be fitted either to Eq. (7) or (8). We found that for all the alloys the second fit was decisively better than the first. In Fig. 2 we show the results of such a fit. Considering the uncertainties involved in extracting the single-particle term, the straight lines seem to be remarkably good. The slope of the straight lines gives the coefficient B of the Stoner term. In Table III we give the results of such an analysis. For comparison, data for pure Ni and one Ni-Fe alloy¹⁴ are also included. No such analysis could be performed for sample no. 51 since the corresponding neutron-scattering data for D_0 are not available. However, the values of B given in this table should be used with a little caution for the following reasons:

(i) Since our experimental results could not resolve whether the next-higher-order term in the spin-wave contribution comes through a $T^{7/2}$ or a T^4 term, the absolute value of $(\gamma)_{\text{expt}}$ is slightly uncertain. This value was subsequently used to estimate $(\gamma)_{\text{SW only}}$.

(ii) Some systematic errors also appeared in estimating the neutron-scattering D_0 values for our alloys from the data of Men'shikov *et al.*³ Such errors could be appreciable because of the sensitive dependence of D_0 on the Cr concentration.

Although the absolute values of B are somewhat uncertain, a few broad but definite qualitative features could be identified. From a comparison of the B values for the alloys with increasing Cr concentration but with approximately the same Fe content, it is quite clear that the addition of Cr enhances the Stoner term considerably. However, the change of B with increasing Fe concentration is

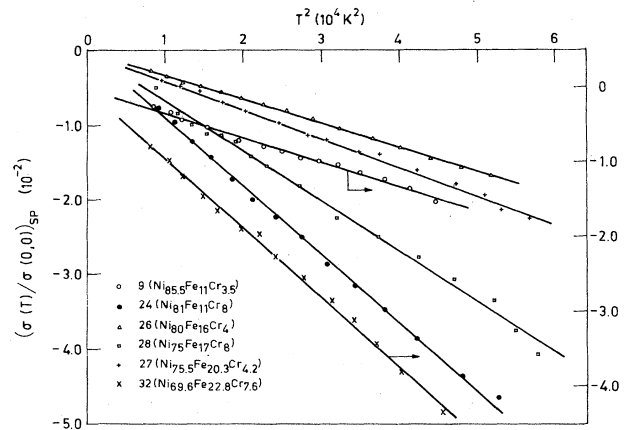


FIG. 2. Change of reduced magnetization $[(\Delta\sigma/\sigma)_{\text{SP}}]$ due to the other than spin-wave excitations, plotted against T^2 for various Ni-Fe-Cr alloys. The solid lines are the best fits according to Stoner's theory of single-particle excitations.

not very clear. Since the value of B is sensitive to Cr concentration, a meaningful comparison of B for the alloys with different Fe concentrations can only be possible when their Cr contents are exactly the same. Even then it can be safely concluded that the change of B with Fe concentration is much less compared to that with Cr.

It is evident from the above analysis that Stoner excitations corresponding to weak itinerant-electron ferromagnets can account for the difference between the magnetization and the neutron-scattering-determined values of D_0 . At the same time it can be also pointed out that the existence of a Stoner term in the low-temperature excitation of a ferromagnet is not sufficient proof that the system is a weak itinerant-electron ferromagnet, because such a term has also been observed in Ni,^{13,14,22} although from de Haas-van Alphen measurements²⁸ it appears to be a strong itinerant-electron ferromagnet. There are other criteria which should be satisfied before one arrives at a conclusion regarding the strong or weak itinerant-electron magnetic behavior in a particular material. However, from the rapid increase of the Stoner term with increasing Cr concentration, and the similarity of this behavior with Ni-Fe (Ref. 15) alloys in the Invar region or those of Fe-

TABLE III. Results of the least-squares fit of $[\Delta\sigma(T)/\sigma(0)]_{\text{SP}}$ to single-particle excitations [Eq. (8)].

Sample no.	Composition of Ni-Fe-Cr alloys (at. %)	B (10^{-7} K^{-2})	Standard deviation of least-squares fit of $[\Delta\sigma(T)/\sigma(0)]_{\text{SP}}$ (10^{-4})
	100-0-0	2.8 ^a (3.2) ^b	
	89.8-10.2-0	1.12 ^a	
9	85.5-11-3.5	3.3	4.0
24	81-11-8	9.1	6.2
26	80-16-4	3.2	1.9
28	75-17-8	6.8	12
27	75.5-20.3-4.2	3.9	4.7
32	69.6-22.8-7.6	9.4	6.4

^aReference 14.

^bFrom Ref. 22.

Pt and Fe-Pd alloys²⁹ (which are all weak itinerant-electron ferromagnets), one might infer that addition of Cr in Ni-Fe alloys shifts it more towards weak itinerant-electron ferromagnetism. Further evidence in support of this idea will be presented and discussed in Sec. III E.

B. Low-temperature magnetization data for Ni-Fe-V alloys

A few alloys in the ternary Ni-Fe-V system were selected for spin-wave study, mainly to see the effect of the addition of vanadium and also the influence of increasing Fe concentration. The choice of alloys was again limited by the same considerations made for the alloys in the Cr system. Similar to Ni-Fe-Cr alloys, the magnetizations as a function of temperature in a constant applied field of 7 kOe were measured, and a computer fit of the data was tried for $T^{3/2}$ and higher-order terms.

In searching for the higher-order terms, two kinds of least-squares fits were tried: (i) with $\sigma(0,0)$, α , and β (coefficient of $T^{5/2}$ term), and (ii) with $\sigma(0,0)$, α , and γ (coefficient of T^4 term). Although the second kind of fit was found to be generally better than the first, the difference ($\sim 5\%$ SD) was found to be marginal. This is in contrast to Ni-Fe-Cr alloys, where the second kind of fit was always convincingly better than the first. Thus there is a possibility that the term β is not negligibly small compared to γ in ternary vanadium alloys.

In Table IV we show the results of the least-squares fits with different higher-order terms, along with the standard deviations. Using the values of α , the spin-wave-stiffness constants D_0 were calculated; they are also included in the table. The values of ρ were calculated in the same manner as discussed earlier, using our measured lattice-parameter values.

Figure 3 shows the change in reduced magnetization with temperature in a constant field of 7 kOe for some Ni-Fe-V alloys; the solid curves are the computer fits with the $T^{3/2}$ term along with the T^4 term. Although the fits seem to be fairly good, in the absence of any neutron-scattering data for D_0 , it could not be ascertained whether the magnetization-derived values for D_0 are the actual ones. However, the Curie temperatures for Ni-Fe-Cr and Ni-Fe-V alloys with about the same concentration of Cr (or V) are of the same order. Since basically both T_c and D_0 are related to the average exchange interaction, it is not altogether unjustified to expect that the D_0 values for vanadium alloys should be of the same order as the corresponding Ni-Fe-Cr alloys. A comparison of our D_0 values for Ni-Fe-V alloys with those of Ni-Fe-Cr alloys (Table II), however, suggests that magnetization-derived D_0 values are much smaller than expected for this system as well. This immediately raises the question of whether, in Ni-Fe-V alloys, do we also have other than spin-wave (possibly Stoner-type) excitations at low temperatures. The similarity of the magnetic behaviors (see Sec. III E) in the two systems strongly favors this viewpoint. The real picture can only emerge when the neutron-scattering data or more precise magnetization data are available.

The other features, e.g., a rapid decrease of D_0 with V concentration in contrast to a smaller one with Fe concen-

TABLE IV. Results of the least-squares fits for the temperature variation of magnetization for some Ni-Fe-V alloys. The statistical uncertainties in the various parameters are also included.

Sample no.	Composition of Ni-Fe-V alloys (at. %)	Density ρ^a (g/cm ³)	$\sigma(0,0)$ (emu/g)	$-\alpha$ ($10^{-5} \text{ K}^{-3/2}$)	$-\beta$ ($10^{-8} \text{ K}^{-5/2}$)	$-\gamma$ (10^{-12} K^{-4})	D_0 (meV \AA^2)	D_2 ($10^{-7} \text{ K}^{-5/2}$)	Standard deviation of least-squares fit of $\Delta\sigma/\sigma$ (10^{-4})
31	74-22-4	8.56	90.2±0.08	1.27±0.13	0.61±0.4	0.6±0.3	199	0.3	4.7
			90.3±0.06	1.39±0.05			187		4.8
30	79.4-17-3.6	8.62	79.2±0.05	1.02±0.1	2.0±0.4	2.9±0.5	250	3.3	3.8
			79.3±0.03	1.33±0.04			209		3.7
18	85-11-4	8.69	61.8±0.02	1.27±0.04	2.9±0.13	3.3±0.15	253	1.2	2.0
			62.0±0.01	1.80±0.02			200		1.9
19	83-10-7	8.65	53.6±0.07	3.01±0.17	4.8±0.6	5.7±0.6	157	1.0	8.7
			53.8±0.04	3.81±0.06			134		7.5

^aCalculated values.

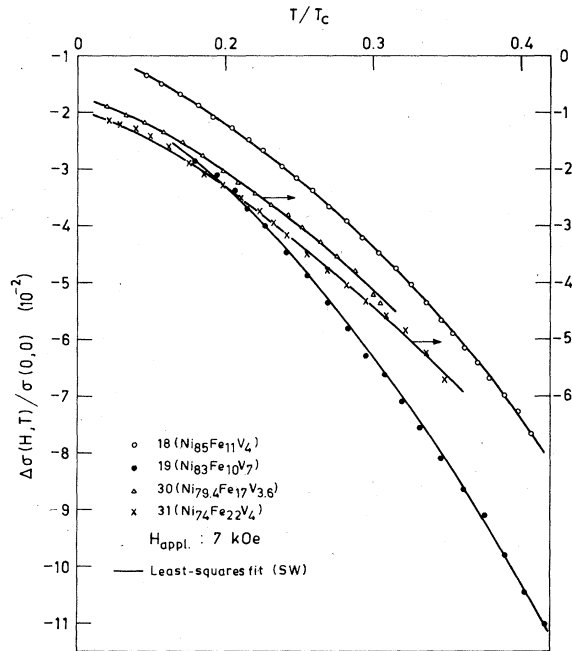


FIG. 3. Same kind of plots as in Fig. 1 for several Ni-Fe-V alloys.

tration, are similar to those of Ni-Fe-Cr alloys. The temperature-dependent part of the spin-wave-stiffness constant (D_2) also shows a decrease with the addition of vanadium.

C. Average number of Bohr magnetons per atom ($\bar{\mu}$)

By extrapolation of the magnetization data (77 K and above) to low temperatures, one can obtain the magnetic moment at 0 K and, thereby, the average number of Bohr magnetons per atom, $\bar{\mu}$. This procedure is fairly simple and accurate for the alloys with higher T_c and those for which spin-wave analysis of magnetization data has been

done. For the alloys with lower T_c (< 450 K), a $T^{3/2}$ magnetization dependence was observed (although over a limited temperature range) above 77 K, which justified the extrapolation procedure even for them. This is because of the fact (as discussed in Secs. IIIA and IIIB) that the alloys with higher Cr (or V) content (lower T_c) show a $T^{3/2}$ dependence over a higher-temperature range in the rationalized scale (T/T_c). However, this extrapolation procedure is unreliable for alloys with a T_c lower than room temperature, and hence no such data will be included here. We estimate that the total error in $\bar{\mu}$ is less than 2% for the first method of analysis and is a little more for the second.

An attempt was made to explain these data in terms of the virtual-bound-state theory of Friedel,³⁰ extended to ternary alloys. Since the addition of Cr (or V) in Ni splits a state above the Fermi level of Ni, and assuming that the variation of $\bar{\mu}$ with concentration in the ternary alloys follows the same logic as in the corresponding binary alloys, one should expect it to satisfy the relationship

$$\bar{\mu} = 0.61 + 2C_{Fe} - (10 + Z)C_M, \quad (9)$$

where C stands for the concentration and Z ($= -4$ for Cr and -5 for V) is the valence difference between Ni and M (M denotes Cr, V, etc.).

Although $\bar{\mu}$ in Ni-Fe-Cr alloys has been extensively studied by Men'shikov and Teplykh,¹ we once again present the same data in Table V for the alloys used in the present study, since the composition of most of them is different from those of the earlier study. Also included are the values of $\bar{\mu}$, as expected from Eq. (9), along with those estimated from the data of Men'shikov and Teplykh.¹ Considering the uncertainties involved in the interpolation procedure, one can easily see that the two sets of data are in fairly good agreement, but the disagreement with Eq. (9) is too strong to be ignored. The fact that our experimental values are always larger than the theoretical values, and that the disagreement between theory and experiment is more for the alloys with higher

TABLE V. Average number of Bohr magnetons per atom, $\bar{\mu}$, and T_c for various Ni-Fe-Cr alloys.

Sample no.	Composition of Ni-Fe-Cr alloys (at. %)	T_c (K)	$\bar{\mu}$			Z_{eff}
			Present data	Data of Men'shikov <i>et al.</i>	According to Eq. (9)	
9	85.5-11-3.5	620	0.68 ± 0.01^a	0.70	0.62	4.3
24	81-11-8	470	0.55 ± 0.01^a	0.57 ^c	0.35	3.5
29	75.1-12.8-12.1	365	0.46 ± 0.015^b	0.45	0.14	3.4
26	80-16-4	693	0.82 ± 0.015^a	0.82	0.69	2.8
28	75-17-8	543	0.68 ± 0.01^a	0.70 ^c	0.47	3.4
33	68.1-17.4-14.5	320	0.48 ± 0.015^b	0.48	0.09	3.3
35	76.8-21.2-2	778	0.96 ± 0.015^b	0.98	0.91	3.7
27	75.5-20.3-4.2	717	0.89 ± 0.015^a	0.89	0.76	3.0
32	69.6-22.8-7.6	635	0.82 ± 0.015^a	0.83	0.61	3.2
51	67-21-12	470	0.63 ± 0.015^a	0.64	0.31	3.3

^aData obtained by spin-wave analysis.

^bData obtained by extrapolation, using $T^{3/2}$ law.

^cValues directly from Ref. 1.

Cr content, might lead one to suspect whether the value 6 taken for $(10+Z)_{Cr}$ is rather too large. The corresponding value of 5.1 ($=d\bar{\mu}/dc|_{Cr}$),³¹ even in binary Ni-Cr alloys, further strengthens this suspicion. To check this, our experimental values of $\bar{\mu}$ were fitted to Eq. (9), replacing $10+Z$ by a variable parameter Z_{eff} . The values of Z_{eff} thus obtained are shown in Table V. It is clear from our analysis that (i) Z_{eff} is much smaller than the ideal value of 6 for the alloys, and (ii) Z_{eff} , instead of being a constant, is itself composition dependent. One should bear in mind, however, that the above analysis was confined to the Ni-rich region only, with the total Fe + Cr concentration never exceeding 30 at. %. However, when one looks into the more comprehensive data of Men'shikov and Teplykh (Fig. 2 of Ref. 1), a strong non-linearity (implying that Z_{eff} is composition dependent) is also observed in the $\bar{\mu}$ -versus-concentration (Fe) curves. Deviation from linearity is more prominent for the alloys with higher Cr concentration. It should also be noted that when we replotted their data for $\bar{\mu}$ as a function of C_{Cr} for a series of alloys with constant Fe content, we found that the rate of decrease of $\bar{\mu}$ with Cr concentration slows down as more and more Cr is added. In other words, Z_{eff} is smaller for the alloys with higher Cr content. Except for a few exceptions (probably due to some uncertainties in determining actual compositions), in general our data also show similar trend. It should also be pointed out that in the later work on binary Ni-Cr alloys by Acker and Huguenin,³² Z_{eff} has been found to decrease with increasing Cr concentration. Men'shikov and Teplykh¹ have tried to explain $\bar{\mu}(c)$ on the basis of "defect theory." When Cr atoms enter a Ni matrix, some of the nearest Ni neighbors try to compensate for the spin-density around Cr atoms which arises because of the different number of "upward" and "downward" spins of the host and the impurity. This causes a magnetic defect in N , the number of nearest Ni neighbors, reducing the total magnetization by $(N+1)0.4=5.2\mu_B/\text{atom}$ ($N=12$ for the fcc lattice, and 0.4 is the magnetic moment of pure Cr). The addition of Fe attempts to suppress the negative spin-polarization effect of Cr atoms. Thus, the opposite roles played by the two kinds of impurities in Ni might provide some qualita-

tive argument in favor of the nonlinear dependence of average magnetic moment on concentration (Fe or Cr). According to this theory, however, increasing Cr concentration should gradually diminish the role played by the Fe atoms, and hence one should expect Z_{eff} to increase with increasing Cr concentration. This is contrary to what we observe from our data, as well as from that of Men'shikov and Teplykh.¹ Therefore this aspect of the problem does not seem to fit the "defect theory." We believe, some coherent-potential-approximation—(CPA-) type calculations for the band structure of this ternary system will be able to explain these data.

In Table VI we present the values of $\bar{\mu}$ from both experiment and theory [Eq. (9)] for some Ni-Fe-V alloys. It can be seen that Eq. (9) again fails to explain the experimental results. To obtain an estimate of Z_{eff} , the same kind of analysis as in Cr alloys has been done. It appears that the average $Z_{eff}=3.8$, instead of 5, and is itself a function of composition, implying nonlinearity in the $\bar{\mu}$ -versus-concentration curves. Thus, essentially the results are similar to those of Ni-Fe-Cr, except for the fact that deviation of Z_{eff} from the ideal value (5) is less for the V system than that for Cr. For small V concentrations, the Z_{eff} are almost near the ideal value of 5, and then start to decrease with increasing V content. This is in contrast to the behavior of $d\bar{\mu}/dc$ in binary Ni-V alloys³² where the Z_{eff} have been found to increase with increasing V concentration (from an initial value of 5 to about 5.7 for $C_V=8$ at. %).

D. Temperature variation of spontaneous magnetization

The spontaneous magnetization (M_S) was measured from 77 K to the respective Curie temperatures of a few alloys in both ternary series. As discussed in the preceding sections (III A and III B), due to a rapid decrease of the spin-wave-stiffness constant with the addition of Cr or V, magnetization in these systems falls off much faster than in Ni or binary Ni-Fe alloys at low temperatures. Thus it appeared interesting to study M_S over the complete ferromagnetic temperature range, at least for a few

TABLE VI. Average number of Bohr magnetons per atom, $\bar{\mu}$, and T_c for various Ni-Fe-V alloys.

Sample no.	Composition of Ni-Fe-V alloys (at. %)	T_c (K)	$\bar{\mu}$		Z_{eff}
			Present data	According to Eq. (9)	
46	82.5-7.5-10	362	0.44 ± 0.015^a	0.26	3.2
19	83-10-7	486	0.56 ± 0.01^b	0.46	3.6
20	80.5-10.5-9	417	0.52 ± 0.01^a	0.37	3.3
18	85-11-4	609	0.65 ± 0.01^b	0.63	4.5
39	77.4-11.9-10.7	393	0.48 ± 0.015^a	0.31	3.4
37	80.9-14.0-5.1	640	0.65 ± 0.015^a	0.63	4.8
38	76.5-14-9.5	462	0.55 ± 0.01^a	0.41	3.6
36	81-17-2.0	746	0.85 ± 0.015^a	0.85	5.0
30	79.4-17-3.6	691	0.82 ± 0.015^b	0.77	3.6
31	74-22-4	741	0.93 ± 0.02^b	0.85	3.0

^aValues obtained by extrapolation, using $T^{3/2}$ law.

^bSpin-wave-analyzed value.

Cr- or V-rich alloys. The similarities in some low-temperature aspects of the magnetization with those of metallic glasses (viz., validity of the $T^{3/2}$ law over a large temperature range) also raised the possibility of some such similarities in the high-temperature behavior.

At temperatures below about $0.8T_c$, spontaneous magnetizations at any temperature were obtained by extrapolation to zero field of the high-field straight-line part of the magnetization-versus-magnetic-field isotherms. At higher temperatures, the well-known Arrott³³ plots (M^2 -versus- H/M isotherms) were used to obtain M_S . Now, according to molecular-field theories, reduced-magnetization-versus-reduced-temperature curves are expected to roughly follow Brillouin functions, except at very low temperatures (due to spin waves) and near the critical region, because of the inherent limitations of these theories. Figure 4 shows the typical experimental results for some Ni-Fe-Cr alloys along with the Brillouin-function curves corresponding to $S=1$, shown by the dotted lines. The behavior of the corresponding V alloys is also essentially similar (not shown in the figure). It can be readily seen that, for all the alloys, magnetization falls much faster than predicted by the theory over the entire temperature range studied. The theoretical curves for $S=\frac{1}{2}$ have not been shown in the figure, partly to preserve clarity and partly because the disagreement with experimental data would have been greater for them. Another aspect of our data, as can be seen from the figure, is that the disagreement between theory and experiment increases with increasing Cr or V concentration.

It is well known that, although approximate, molecular-field theories with $S=\frac{1}{2}$ and 1 can explain fairly well the magnetization data of crystalline Ni and Fe, respectively, within their limitations. It appears, how-

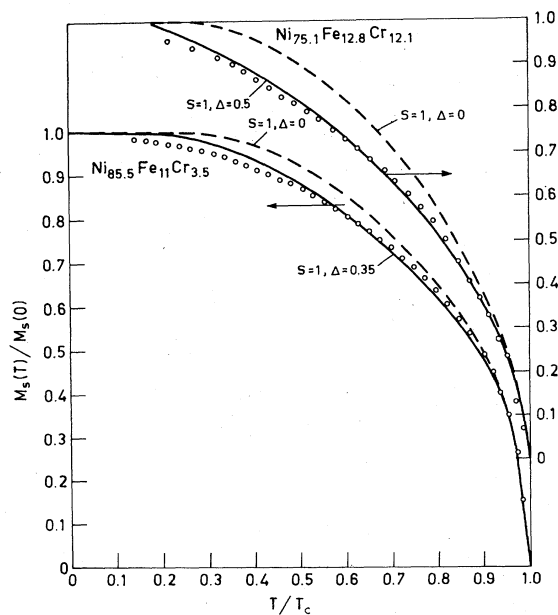


FIG. 4. Reduced spontaneous magnetization vs reduced temperature for two Ni-Fe-Cr alloys. Dotted lines correspond to Brillouin functions and solid lines to modified Brillouin functions for $S=1$ (see text).

ever, that this kind of theory is rather inadequate for the present systems. As pointed out in Secs. IIIA and IIIB, the dominance of a large spin-wave contribution to the decrease of magnetization up to fairly high temperatures ($\sim 0.5T_c$) could be a plausible reason for the disagreement at low temperatures. However, such an argument cannot be extended to treat the disagreement at higher temperatures. In this context it is also interesting to point out that such "diminished curvature" of the magnetization behavior has also been observed in the recent studies of metallic glasses,^{34,35} and has been explained on the basis of a theory proposed by Handrich.³⁶ The basic idea is that in the presence of disorder the molecular field varies in a random manner from site to site, and hence the reduced magnetization is related to the modified Brillouin functions³⁶

$$M_S(T)/M_S(0) = \frac{1}{2} [B_S(1+\Delta)x + B_S(1-\Delta)x], \quad (10)$$

where

$$x = [3S/(S+1)][M_S(T)/M_S(0)],$$

and Δ is a measure of disorder, defined as the rms deviation from the average exchange interaction between nearest-neighbor pairs. In the absence of any disorder, Eq. (10) is reduced simply to $B_S(x)$, as expected. Therefore it was natural to try Eq. (10) with Δ as a parameter to fit our experimental data. In Table VII we present the values of Δ for both $S=1$ and $\frac{1}{2}$ corresponding to the best fits. The solid curves in Fig. 4 are the best-fitted ones for $S=1$ and are tolerably good if the limitations of the theory are kept in mind. It is clear from the table that whatever the value of S ($\frac{1}{2}$ or 1), Δ always increases with the addition of Cr or V for an alloy series with fixed Fe concentration. When Fe concentration is increased, maintaining Cr concentration fixed, however, Δ changes very slightly. An increase of Fe concentration by about 8 at. % has reduced Δ only by about 0.05 for both $S=1$ and $\frac{1}{2}$, but the corresponding increase of Cr resulted in a change of Δ by 0.15. In the case of V the changes are smaller. Now since Δ is a measure of disorder, the implication of the above results is that the addition of Cr or V in these ternary systems drastically increases disorder, whereas the addition of Fe has very little effect; if at all, it tries to suppress disorder. The important question is what kind of disorder can arise from the addition of Cr or V. Since these are all polycrystalline materials, one can rule out the possibility of any structural disorder, but there is a dis-

TABLE VII. Results of best fits of the reduced-magnetization data to modified Brillouin functions.

Sample no	Composition (at. %)	Values of Δ for best possible fit with	
		$S=1$	$S=0.5$
9	Ni _{85.5} Fe ₁₁ Cr _{3.5}	0.35	0.4
29	Ni _{75.1} Fe _{12.8} Cr _{12.1}	0.5	0.55
51	Ni ₆₇ Fe ₂₁ Cr ₁₂	0.45	0.5
19	Ni ₈₃ Fe ₁₀ V ₇	0.4	0.45
39	Ni _{77.4} Fe _{11.9} V _{10.7}	0.5	0.5

tinct possibility of higher "magnetic disorder" (implying the random nature of the exchange interaction), especially in the case of Ni-Fe-Cr alloys because of the large antiferromagnetic interaction³ between Cr atoms.

Thus if one follows the disorder approach, even localized theories can explain the magnetization behavior of the two ternary systems. However, there is another possibility (as will be discussed in the next section), namely that all these anomalies arise simply because the Cr- or V-rich alloys behave more as weak itinerant-electron ferromagnets.

E. Itinerant-electron versus localized model

The magnetization behavior studied so far reveals two interesting features. (i) A rapid increase of the Stoner (T^2) term in magnetic excitation with the addition of Cr in Ni-Fe alloys. Although the presence of such a term could not be established in Ni-Fe-V alloys, our low-temperature magnetization measurements still gave some indication about the presence of additional excitations other than spin waves. (ii) Reduced magnetization for alloys in both ternary systems falls much faster with temperature than predicted by molecular-field theories, and this discrepancy widens with increasing concentration of Cr or V. These facts, along with the nonintegral values of average number of Bohr magnetons/atom ($\bar{\mu}$) and their nonlinear dependence on concentration, opened up the possibility of a suitable explanation of our data in the framework of itinerant-electron models (IEM's) rather than the localized ones.

In the last 20 years some useful criteria have been developed by Wohlfarth and co-workers to distinguish between materials obeying localized models (LM's) and those following IEM's. One of them is the Rhodes-Wohlfarth plot,^{37,38} where the ratio q_c/q_s is related to the Curie temperature T_c . Here, q_s is the average number of Bohr magnetons per atom derived from the low-temperature magnetization data, and q_c is the corresponding quantity derived from the Curie-Weiss constant (C) in the paramagnetic region by using the relationship

$$C = \frac{N\mu_B^2 p_{\text{eff}}^2}{3k_B}, \quad (11)$$

where

$$p_{\text{eff}}^2 = q_c(q_c + 2), \quad (12)$$

N is the number of atoms/g, and k_B is the Boltzmann constant. The basic philosophy of the Rhodes-Wohlfarth plot is that in the case of localized electrons the effective spin is the actual spin, and hence $q_c/q_s = 1$ for all T_c . In the case of itinerant electrons, however, q_s might be less than the maximum possible value, and hence $q_c/q_s > 1$. This ratio will be larger, the weaker the ferromagnetism, and hence should be related to T_c by

$$q_c/q_s \propto T_c^{-1}. \quad (13)$$

It has been shown³⁸ that this kind of plot for a large number of alloys and compounds with diverse constituents shows a systematic trend of increasing with decreas-

ing T_c [if not following the same universal curve as predicted by Eq. (13)]. However, the Curie-Weiss behavior above T_c , though observed in almost all ferromagnets including weak itinerant-electron systems such as ZrZn₂ (Refs. 39 and 40) and Sc₃In (Ref. 41), finds little support from the Stoner²⁴ model or from its later extension by Edwards and Wohlfarth.⁴² In the limit of very weak ferromagnetism, Edwards and Wohlfarth show that

$$X = X_0 \left[1 - \frac{T^2}{T_c^2} \right]^{-1}, \quad T < T_c \quad (14)$$

$$X = 2X_0 \left[\frac{T^2}{T_c^2} - 1 \right]^{-1}, \quad T_F > T > T_c$$

where T_F is the effective degeneracy temperature of the fermion system above which the Pauli exclusion principle can no longer restrict the occupation of the bands as all electrons or holes around E_F are thermally excited, and X_0 is the differential susceptibility at 0 K, given by

$$X_0 = Nn(E_F)\mu_B^2 / [In(E_F) - 1], \quad (15)$$

where N is the number of atoms, $n(E_F)$ is the density of states per atom per spin at E_F , and I is the exchange parameter. Thus, according to the Edwards-Wohlfarth theory, $X^{-1} \propto T^2$. However, this has not been observed in any weak ferromagnetic system, except Ni₃Al.⁴³ Curie-Weiss (CW) behavior, according to Wohlfarth,⁴⁴ is expected only when $T \gg T_F$, which is definitely not the case in the temperature ranges where CW behavior has been observed in ZrZn₂ or other similar systems. The failure of these theories to explain the observed CW behavior naturally points to the inadequacy of Hartree-Fock approximations, on which these theories were based and developed to describe finite-temperature properties, even for very weak ferromagnets. Hence, although from a theoretical point of view deduction of local moments from the Curie constant is questionable, the ratio q_c/q_s nevertheless serves as an useful indicator for the degree of itinerancy.

In this regard it seems relevant to add that although the CW behavior is not explained by these theories, the dynamical "spin-fluctuation" approach by Moriya and Kawabata⁴⁵ can explain them very well through an entirely different mechanism. A unified approach in terms of spin-density fluctuations has also been suggested²⁶ to explain the properties of materials which lie between the two extremes (localized and weak itinerant-electron limits) and whose q_c/q_s ratios lie between the two (1 and ∞).

Thus we may conclude from the above discussions that measurements of paramagnetic susceptibility can serve a useful purpose in determining the itinerant-electron or localized character of magnetism. Our measurements in the ferromagnetic region for both ternary systems showed some indication of behaving like weak itinerant-electron systems. To check this, paramagnetic susceptibility measurements were carried out for three alloys in the Ni-Fe-Cr system and two in Ni-Fe-V. Out of the five samples, two of them (one in each series) have a T_c below room temperature. Even for them, measurements were carried out only above room temperature. This is partly because

the other three alloys studied showed pure paramagnetic behavior at temperatures far above T_c (only above $T - T_c > 100$ K). The deviation from pure paramagnetic behavior, characterized by the nonlinear relationship between M and H , is probably due to some kind of short-range order or some superparamagnetic clusters present at temperatures well above T_c . Figure 5 shows some characteristic M -versus- H graphs above T_c .

In Fig. 6 we show inverse susceptibility as a function of temperature measured in a constant field of 5 kOe for the alloys under discussion. All the alloys show fairly well-defined CW behavior from a temperature high above their respective T_c 's to the highest temperature of the measurements. The slope of the straight line gives the inverse of the Curie-Weiss constant ($1/C$), and its intercept on the temperature axis gives Θ , the paramagnetic Curie temperature. The values of q_c for the respective alloys were calculated using Eq. (12) and our experimentally determined values of C^{-1} . In Table VIII we present the results of such calculations, along with the values of T_c , Θ , and also T_d , the temperature at which a deviation from CW law is observed, for the various alloys under consideration. The values of q_s were taken from Tables V and VI (actually, $q_s = \bar{\mu}$ given in these tables) for sample nos. 24, 29, and 19, and the corresponding quantity for sample nos. 45 and 48 were estimated from compositions close to them. For comparison, q_c and q_s values for some typical weak itinerant-electron ferromagnets are also included in Table VIII. It is quite apparent from the table that q_c/q_s indeed shows a systematic increase with decreasing T_c , i.e., with increasing concentration of Cr or V. The values are also comparable to the literature values of

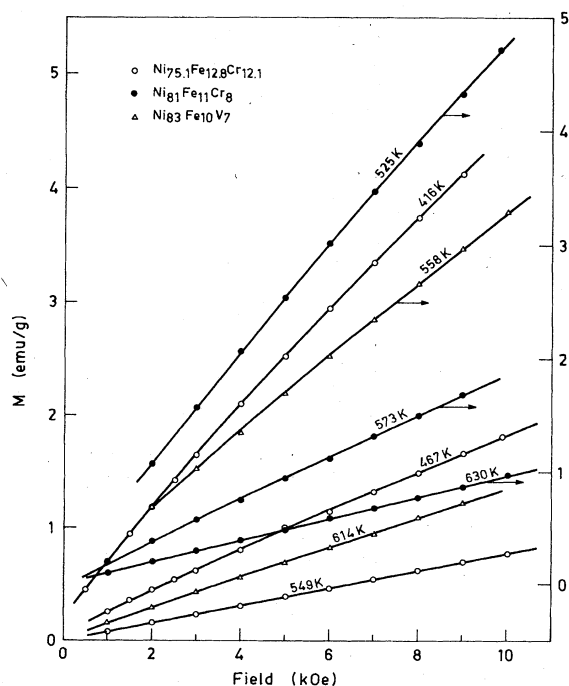


FIG. 5. Magnetization—vs—applied-magnetic-field isotherms at several temperatures above the respective Curie temperatures for some Ni-Fe-Cr (or -V) alloys.

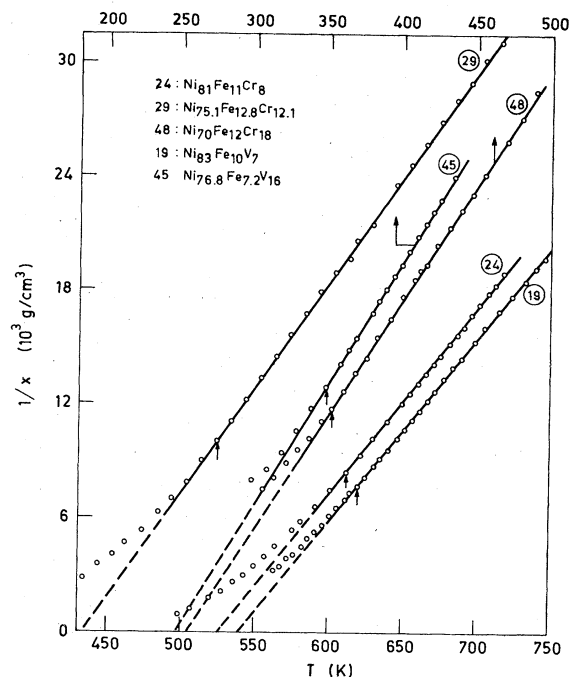


FIG. 6. Reciprocal susceptibility vs temperature above T_c for several Ni-Fe-Cr (or -V) alloys.

some binary and ternary alloys of different constituents which have T_c values close to those of our alloys. It should also be noted that our q_c/q_s values for Ni-Fe-Cr alloys are nearly the same as those for Ni-Fe-V alloys with comparable T_c 's. Such experimentally observed systematic behavior lends strong support to the contention that the addition of Cr or V to Ni-Fe alloys drives them more towards itinerant-electron weak ferromagnetism. This is in contrast to the case of binary Ni-Fe alloys, which show strong itinerant-electron behavior in the Ni-rich region and weak itinerant-electron behavior in the Invar region.¹⁴

One striking feature of all the alloys is the large difference between paramagnetic and ferromagnetic Curie temperatures, Θ and T_c . It can also be seen from Table VIII that the difference $\Theta - T_c$ increases with increasing concentration of Cr or V. Such large differences have also been observed in Cr-rich Fe-Cr alloys (see Table VIII). Similarly, the temperature from which the deviation from Curie-Weiss behavior starts (T_d), also increases with increasing Cr or V concentration. This behavior was also reflected in the M -versus- H isotherms above T_c , as discussed earlier. For all the alloys, T_d was found to be close to the temperatures where the M -versus- H isotherms show perfect linearity. Recently, Moriya⁴⁹ has shown that in weak itinerant-electron systems strong short-range order might persist even up to temperatures much higher than T_c . The fact that in sample nos. 45 and 48 short-range order persists even up to $2T_c$ probably finds some theoretical support from his theory.

Materials with weak itinerant-electron character (large q_c/q_s) should also show a host of other properties, viz., their Arrott plots should be a set of parallel straight lines

TABLE VIII. Values of T_c , Θ , T_d , q_c , and q_s for some Ni-Fe-Cr (or -V) alloys.

Sample no.	Alloy composition (at. %)	T_c (K)	Θ (K)	T_d (K)	q_c (μ_B)	q_s (μ_B)	q_c/q_s
24	Ni ₈₁ Fe ₁₁ Cr ₈	470	526	612	1.39	0.55	2.5
29	Ni _{75.1} Fe _{12.8} Cr _{12.1}	365	434	524	1.27	0.46	2.8
48	Ni ₇₀ Fe ₁₂ Cr ₁₈	179	255	352	1.19	0.30 ^a	4.0
19	Ni ₈₃ Fe ₁₀ V ₇	486	540	620	1.41	0.56	2.5
45	Ni _{76.8} Fe _{7.2} V ₁₆	167	248	348	1.14	0.27 ^a	4.2
	ZrZn _{1.9} ^b	26			0.86	0.16	5.4
	(Fe _{0.3} Ni _{0.7}) ₂ B ^c	307			1.31	0.50	2.62
	(Fe _{0.2} Ni _{0.8}) ₂ B ^c	105			0.85	0.24	3.54
σ phase	Fe _{56.5} Cr _{43.5} ^d	47	60		0.967	0.125	7.7
	Fe _{55.1} Cr _{44.9} ^d	29	53		0.788	0.096	8.2
	Fe _{55.5} V _{44.5} ^d	160	165		1.139	0.222	5.1

^aEstimated values from Table VI and Ref. 1.

^bReference 46.

^cReference 47.

^dReference 48.

over a wide range of temperature.³⁸ Usually, the Arrott plots are found to be straight lines (except for some deviations in the low-field region) for all ferromagnets near T_c . This kind of relationship comes directly from the Landau theory of phase transitions when the free energy is expressed in powers of magnetization³³ in the limit of $M(T)/M(0) \ll 1$ near T_c . The slopes of such plots, however, are temperature dependent. On the other hand, Edwards and Wohlfarth⁴² have shown that in the limit of

very weak ferromagnetism ($\xi_0 \ll 1$, where ξ_0 is the relative magnetization of spin-up and spin-down electrons),

$$\left[\frac{M(H,T)}{M(0,0)} \right]^2 = \left[1 - \left(\frac{T}{T_c} \right)^2 \right] + \frac{2X_0H}{M(H,T)}. \quad (16)$$

Hence the Arrott plots at all temperatures below T_F ($T_c \ll T_F$ for weak systems) should be a set of parallel straight lines with slopes equal to $2X_0[M(0,0)]^2$.

Figure 7 shows the Arrott plots over a wide temperature range for two Ni-Fe-Cr alloys and one Ni-Fe-V alloy for which the susceptibilities were measured. Except for the deviation at low fields, which is naturally expected due to domain orientation and some possible spatial inhomogeneity in the sample, the plots appear as fairly straight lines. However, because of the limited field range available, the number of data points in the linear part, especially at lower temperatures, is small. At higher temperatures, however, the linearity of such plots has been established without any ambiguity. On the other hand, the slopes are definitely not temperature independent, but then, even in ZrZn₂,⁵⁰ which is thought to be almost an ideally weak ferromagnet, the slopes of the Arrott plots show considerable temperature dependence. Thus in our case the temperature dependence of the slope is not altogether unexpected since, by any consideration, these alloys cannot be considered to be perfectly weak ferromagnets. Such behavior has also been observed in Ni-Pt (Ref. 51) and in Fe-Ni (Ref. 52) Invar alloys. Thus, in spite of the temperature dependence of the slope, the linearity of the Arrott plots over a wide temperature range itself verifies the weak itinerant-electron behavior in these systems. In conclusion, all the experimental evidence obtained from the present work points to the fact that the addition of Cr or V in Ni-Fe alloys shifts them gradually towards weak itinerant-electron ferromagnetism.

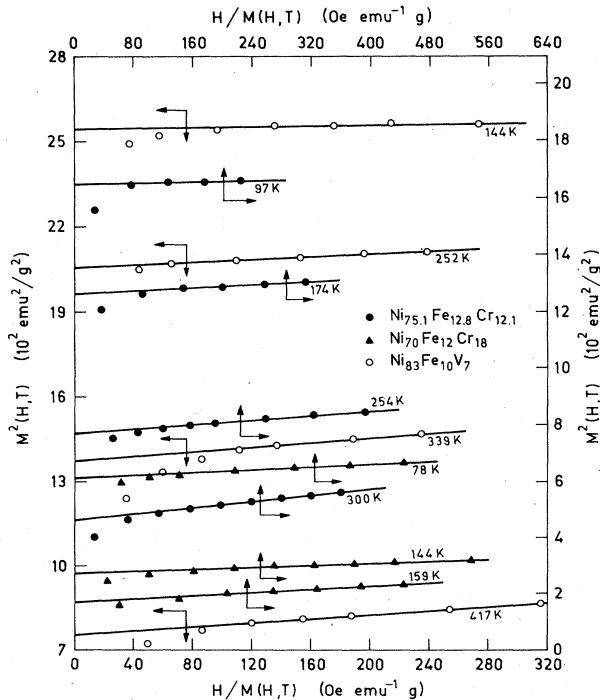


FIG. 7. Arrott plots (M^2 -vs- H/M isotherms) at several temperatures for several Ni-Fe-Cr (or -V) alloys.

- ¹A. Z. Men'shikov and A. Ye. Teplykh, *Fiz. Met. Metalloved.* **44**, 1215 (1977) [*Phys. Met. Metallogr. (USSR)* **44**, 78 (1977)].
- ²A. K. Majumdar and P. v. Blanckenhagen, *Phys. Rev. B* **29**, 4079 (1984).
- ³A. Z. Men'shikov, N. N. Kuzmin, V. A. Kazantsev, S. K. Sidorov, and V. M. Kalinin, *Fiz. Met. Metalloved.* **40**, 647 (1975) [*Phys. Met. Metallogr.* **40**, 174 (1975)].
- ⁴F. Keffer, in *Handbuch der Physik*, edited by S. Flügge (Springer, Berlin, 1966), Vol. XVIII/2.
- ⁵B. E. Argyle, S. H. Charap, and E. W. Pugh, *Phys. Rev.* **132**, 2051 (1963).
- ⁶F. J. Dyson, *Phys. Rev.* **102**, 1217 (1956); **102**, 1230 (1956).
- ⁷J. A. Copeland and H. A. Gersch, *Phys. Rev.* **143**, 236 (1966).
- ⁸T. Izuyama and R. Kubo, *J. Appl. Phys.* **35**, 1074 (1964).
- ⁹J. Mathon and E. P. Wohlfarth, *Proc. R. Soc. London, Ser. A* **302**, 409 (1968).
- ¹⁰M. W. Stringfellow, *J. Phys. C* **1**, 950 (1968).
- ¹¹V. J. Minkiewicz, M. F. Collins, R. Nathans, and G. Shirane, *Phys. Rev.* **182**, 624 (1969).
- ¹²H. A. Mook, J. W. Lynn, and R. M. Nicklow, *Phys. Rev. Lett.* **30**, 556 (1973).
- ¹³A. T. Aldred, *Phys. Rev. B* **11**, 2597 (1975).
- ¹⁴I. Nakai, *J. Phys. Soc. Jpn.* **52**, 1781 (1983).
- ¹⁵I. Nakai, F. Ono, and O. Yamada, *J. Phys. Soc. Jpn.* **52**, 1791 (1983).
- ¹⁶B. Antonini and F. Menzinger, *Solid State Commun.* **9**, 417 (1971).
- ¹⁷M. Hennion, B. Hennion, A. Castets, and D. Tocchetti, *Solid State Commun.* **17**, 899 (1975).
- ¹⁸Y. Ishikawa, S. Onodera, and K. Tajima, *J. Magn. Magn. Mater.* **10**, 183 (1979).
- ¹⁹C. L. Chien and R. Hasegawa, *Phys. Rev. B* **16**, 2115 (1977), and references cited therein.
- ²⁰A. K. Majumdar, V. Oestreich, D. Weschenfelder, and F. E. Luborsky, *Phys. Rev. B* **27**, 5618 (1983).
- ²¹P. C. Riedi, *Phys. Rev. B* **15**, 5197 (1977).
- ²²P. C. Riedi, *Physica (Utrecht)* **91B**, 43 (1977).
- ²³A. T. Aldred, *Phys. Rev. B* **14**, 219 (1976).
- ²⁴E. C. Stoner, *Proc. R. Soc. London, Ser. A* **165**, 372 (1938).
- ²⁵C. Herring in *Magnetism*, edited by G. T. Rado and H. Suhl (Academic, New York, 1966), Vol. IV, Chap. VI.
- ²⁶T. Moriya, *J. Magn. Magn. Mater.* **31-34**, 10 (1983), and references cited therein.
- ²⁷E. D. Thompson, E. P. Wohlfarth, and A. C. Bryan, *Proc. Phys. Soc. London* **83**, 59 (1964).
- ²⁸A. V. Gold, *J. Low Temp. Phys.* **16**, 3 (1974).
- ²⁹O. Yamada, F. Ono, I. Nakai, H. Maruyama, K. Ohta, and M. Suzuki, *J. Magn. Magn. Mater.* **31-34**, 105 (1983).
- ³⁰J. Friedel, *Nuovo Cimento Suppl.* **7**, 287 (1958).
- ³¹M. J. Besnus, Y. Gottehrer, and G. Munsch, *Phys. Status Solidi B* **49**, 597 (1972).
- ³²F. Acker and R. Huguenin, *Phys. Lett.* **53A**, 167 (1975).
- ³³A. Arrott, *Phys. Rev.* **108**, 1394 (1957).
- ³⁴C. C. Tsuei and H. Lilienthal, *Phys. Rev. B* **13**, 4899 (1976).
- ³⁵S. N. Kaul, *Phys. Rev. B* **24**, 6550 (1981), and references cited therein.
- ³⁶K. Handrich, *Phys. Status Solidi* **32**, K55 (1969).
- ³⁷P. Rhodes and E. P. Wohlfarth, *Proc. R. Soc. London, Ser. A* **273**, 247 (1963).
- ³⁸E. P. Wohlfarth, *J. Magn. Magn. Mater.* **7**, 113 (1978).
- ³⁹H. J. Blythe, *Phys. Lett.* **21**, 144 (1966).
- ⁴⁰G. S. Knapp, *J. Appl. Phys.* **41**, 1073 (1970).
- ⁴¹W. E. Gardner, T. F. Smith, B. W. Howlett, C. W. Chu, and A. Sweedler, *Phys. Rev.* **166**, 577 (1968).
- ⁴²D. M. Edwards and E. P. Wohlfarth, *Proc. R. Soc. London, Ser. A* **303**, 127 (1968).
- ⁴³P. F. De Châtel and F. E. DeBoer, *Physica (Utrecht)* **48**, 331 (1970).
- ⁴⁴E. P. Wohlfarth, *J. Appl. Phys.* **39**, 1061 (1968).
- ⁴⁵T. Moriya and A. Kawabata, *J. Phys. Soc. Jpn.* **34**, 639 (1973); **35**, 669 (1973).
- ⁴⁶G. S. Knapp, F. Y. Fradin, and H. V. Culbert, *J. Appl. Phys.* **42**, 1341 (1971).
- ⁴⁷M. C. Cadeville, thesis, University of Strasbourg, 1965.
- ⁴⁸D. A. Read, E. H. Thomas, and J. B. Forsythe, *J. Phys. Chem. Solids* **29**, 1569 (1968).
- ⁴⁹T. Moriya, *J. Phys. Soc. Jpn.* **51**, 420 (1982).
- ⁵⁰S. Ogawa and N. Sakamoto, *J. Phys. Soc. Jpn.* **22**, 1214 (1967).
- ⁵¹H. L. Alberts, J. Beille, D. Bloch, and E. P. Wohlfarth, *Phys. Rev. B* **9**, 2233 (1974).
- ⁵²O. Yamada, F. Ono, and I. Nakai, *Physica (Utrecht)* **91B**, 298 (1977).